Encyclopedia of Polymer Composites

Properties, Performance and Applications

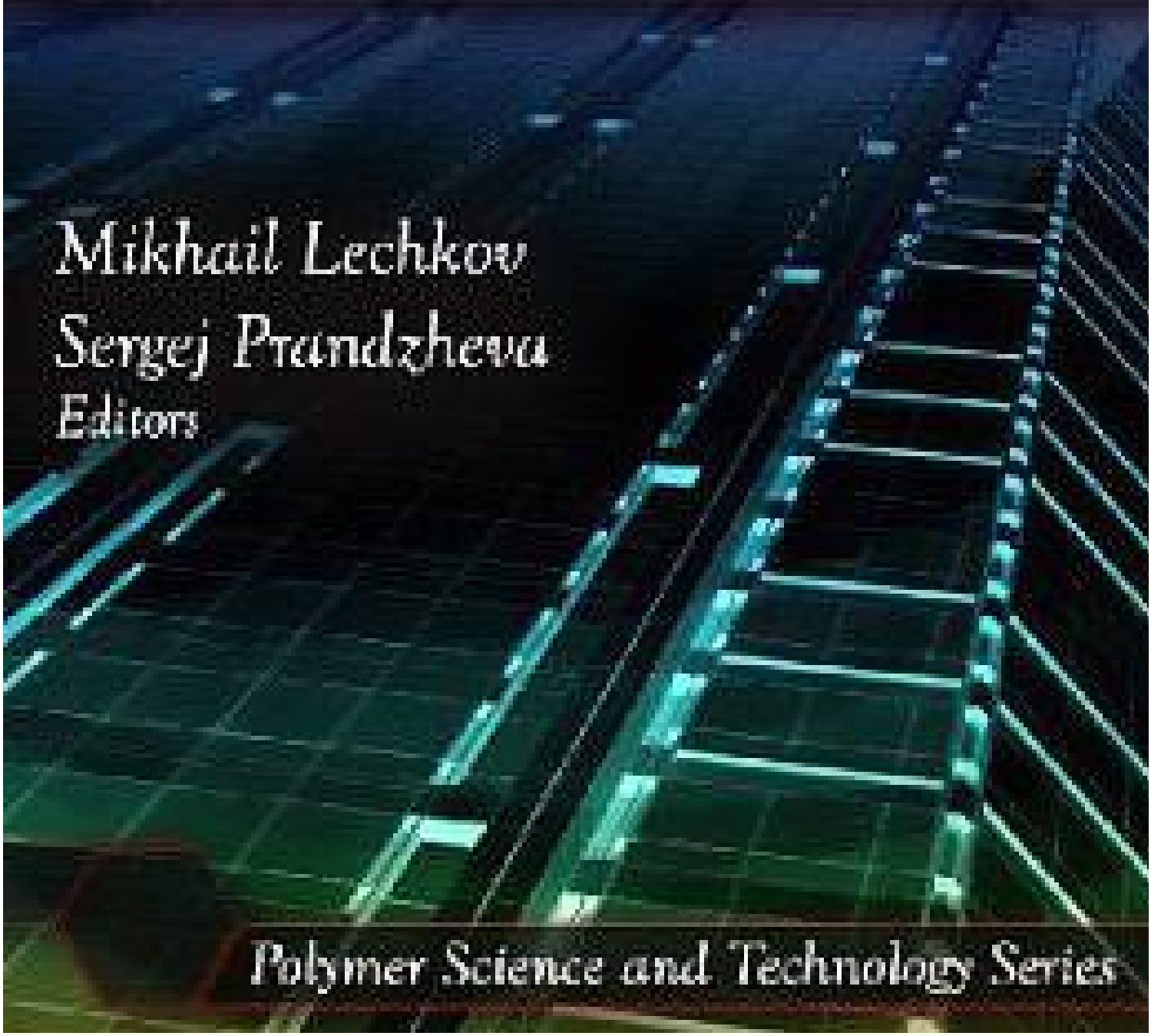

Mikhail Lechkov
Sergej Prandzheva
Editors

Polymer Science and Technology Series

Encyclopedia of Polymer Composites: Properties, Performance and Applications

Mikhail Lechkov and Sergej Prandzheva (Eds.)

In the last several years, polymer composites have been used heavily in the construction sector, such as to repair or design buildings and bridges, strengthen structures and as stand-alone components. About 30% of all polymers produced each year are used in the civil engineering and building industries. In addition to construction, polymer composites are also used in transportation (moulded parts, fuel and gas tanks), aerospace (satellites and aircraft structures), marine, biomedical (dental fixtures, prosthetic devices), electronics and in recreation industries. Such properties associated with polymer composites, in addition to its performance and applications, are continually being researched. Some topics examined in this book include the durability of the base components of FRP (fiber-reinforced polymer), specifically designed for civil engineering industry. The most common environmental agents, mostly responsible for the deterioration of the materials performance are also discussed.

Furthermore, the interfacial adhesion between nanotubes and polymers and the different strategies to promote adhesion are explored to help readers understand the potential and challenges faced by scientists and engineers regarding the use of carbon nanotubes as a reinforcement phase in nanocomposites. This book also reviews the state-of-the-art of syntactic foams and shape memory polymers. The underlying principle for self-heating is also analyzed. Other chapters examine the processing of polymers into antimicrobial materials using polymer/clay nanotechnology, the various methods of synthesis for polyaniline-based nanoparticle-hybrid materials, and the steps towards understanding the complex relationships between specific factors in the production of plastic composites.

Nova Science Publishers Inc.

New York

2010

Table of Contents:

Chapter 11

LIGHT-INDUCED EPR SPECTROSCOPY OF CHARGE CARRIERS PHOTOINDUCED IN POLYMER/FULLERENE COMPOSITES[1]

V.I. Krinichnyi
Institute of Problems of Chemical Physics RAS, Semenov Avenue 1,
Chernogolovka 142432, Russia

ABSTRACT

Composites of conjugated polymers with fullerenes are perspective materials for plastic photovoltaics. In the present Chapter, the Light-Induced EPR (LEPR) study of magnetic, relaxation and dynamic parameters of polaron-fullerene radical pairs photoinduced in bulk heterojunction of various polymer/fullerene composites is described. Weak interaction of positively charged polarons and negatively charged fullerene anion radicals in these radical pairs was shown to stipulate by a difference interaction of charge carriers with own microenvironment. Paramagnetic susceptibility of these radicals reflects their activation dynamics and exchange interaction in the polymer/fullerene system. A decay of long-living spin pairs depends on the spatial distance between photoinduced charge carriers and on the energy of exciting photons. Microwave steady-state saturation method allowed to determine separately all relaxation and dynamics parameters for both type of charge carriers. 1D polaron diffusion along a polymer chain and fullerene pseudorotation near own main molecular axis was shown to follow activation Elliot hopping model and to be governed by photon energy. The energy required for activation of polaron diffusion differs from that of fullerene pseudorotation that proves a noninteracting character of charge carriers photoinduced in polymer/fullerene composites. Main magnetic, relaxation and dynamics parameters of these charge carriers are governed by the photon energy due inhomogeneity of distribution of polymer and fullerene domains in the composite.

[1] This Chapter is dedicated to my parents, Eugenia P. and Ivan Z. Krinichnyi.

1. INTRODUCTION

During the last two decades, research has been increasing in the field of synthesis and characterization of molecules with extended π-electron delocalization considering them as perspective materials for molecular electronics. Among elements of molecular electronics based on conjugated polymers and their composites with fullerenes [1-4] organic plastic solar cells seem to be the most suitable for polymer photovoltaics that at the present time stipulates their wide investigation [3-9].

Plastic solar cells consist of fullerene molecules embedded into conjugated polymer matrix. They form so called bulk heterojunction and perform as electron acceptor (electron transporter, *n*-type material) and as electron donor (hole transporter, *p*-type material), respectively. Soluble conjugated polymers and fullerene derivatives were proved [3, 4, 6, 7, 10-12] to be the most efficient components for the creation of such solar cells. Beyond photoinduced charge exciting and separation, positive carriers are transported to electrodes by polarons diffusing in the polymer phase and electrons hopping between fullerene domains. A definitive advantage of a bulk heterojunction is that it can be made by simply mixing these materials in an organic solvent, and casting with well-known solution deposition techniques, e.g. spin coating [13], the doctor blade technique [14], screen printing [15], or an evaporative spray deposition technique [16]. For the simplicity of their producing, in plastic solar cells are frequently used soluble derivatives of polythiophene, poly(3-alkylthiophene-2,5-diyls) (P3AT) [17-26], and fullerene derivatives with various structure of their side alkyl substitutes [4] as electron donor and electron accepter, respectively.

The irradiation of such bulk heterojunction by visible light with photon energy $h\nu_{ph}$ higher than the π-π* energy gap of the conjugated polymer E_g leads to the formation of ion-radical pair, polaron $P^{+\bullet}$ on a polymer chain (donor, *D*) and $C_{60}^{-\bullet}$ between polymer chains (acceptor, *A*), and charge separation as following [27-29]:

(i) excitation of polaron on polymer chain: $D + A \rightarrow D^* + A$,
(ii) excitation delocalization on the complex: $D^* + A \rightarrow (D–A)^*$,
(iii) initiation of charge transfer: $(D–A)^* \rightarrow (D^{\delta+}–A^{\delta-})$,
(iv) formation of ion-radical pair: $(D^{\delta+}–A^{\delta-})^* \rightarrow (D^{+\bullet}–A^{-\bullet})$, and
(v) charge separation: $(D^{+\bullet}–A^{-\bullet}) \rightarrow D^{+\bullet} – A^{-\bullet}$.

The donor and acceptor units are spatially close but are not covalently bonded. At each step, the *D*–*A* system can relax back to the ground state, releasing energy to the 'lattice' in the form of heat or emitted light. This process revealed by time-resolved spectroscopy occurs in the femtosecond time domain [30-33], whereas the electron backtransfer with charge annihilation is much slower [28] possible due to dynamics and relative slow structural relaxation in such a system of lowed dimensionality [27]. Understanding of photoexcitation, recombination of charge carriers, and other electronic processes realized in conjugated polymers is of fundamental interest for both material characterization and molecular device fabrication.

Bulk heterojunction is characterized by efficient light-excited charge generation at the interface between two organic materials with different electron affinity. Figure 1 illustrates the energy diagram of two intrinsic semiconductors, soluble derivatives of polythiophene and

fullerene, before making a contact between them. A heterojunction formed by these materials inserted between a high work-function electrode (El_1) matching the highest occupied molecular orbital (HOMO) level of the donor and a low work-function electrode (El_2) matching the lowest unoccupied molecular orbital (LUMO) level of the electron acceptor should in principle act as a diode with a rectifying current–voltage characteristics. Under the forward bias (the low work-function electrode is biased negative with respect to the high work-function electrode) the electron injection into the LUMO of the acceptor layer from the low work-function electrode as well as the electron extraction out of the HOMO of the donor by the high work-function electrode are energetically possible and a high current may flow through the heterojunction. Under reverse bias (the low work-function electrode is biased positive with respect to the high work-function electrode), the electron removal from the electron donor and electron injection to the electron acceptor are energetically unfavorable.

Efficiency of light conversion of organic solar cells has overcome the 5% barrier and current efficiency lies within 5 – 6% [9-11]. This parameter is governed by different factors. The first limitation is originated from the high binding energy of polarons photoinduced upon light excitation in conjugated polymers, so by blending in an electron acceptor, it becomes energetically favorable for the electron to escape a polymer macromolecule and to transfer to an acceptor. This requires the LUMO of a donor to be 0.3 to 0.5 eV higher than the LUMO of an acceptor [34, 35]. However, such energy difference can be much higher for some polymer matrices, which decreases optimal open-circuit voltage, since the latter is ultimately limited by the difference between the HOMO of a donor and the LUMO of an acceptor [36, 37]. Raising, e.g. the LUMO of an acceptor it becomes real to increase the efficient factor of plastic solar cells without affecting their light absorption. This approach is theoretically more beneficial for a single-layer solar cell, and results in an estimated efficiency of 8.4% when the LUMO offset is reduced to 0.5 eV [38]. The second constraint comes due to the finite number and mobility of charge carriers in organic solar cells which are lower as compared with those of conventional semiconductors. These main parameters depend on the structure and properties of polymer matrix and fullerene derivative embedded [39-41]. This is a reason why their power-conversion efficiency appears to be governed also by an ultrafast electron transfer from photoexcited polymer chain to fullerene globule [32], a large interfacial area for charge separation due to intimate blending of the materials [13], and efficient carrier transport across a thin film. Unambiguously, to increase power-conversion efficiency it is necessary to photoinitiate a higher density of charge carriers. However, an increased carrier density causes a reduced lifetime due to bimolecular recombination and the efficiency of solar cells might be reduced. Thermal annealing can modify the morphological structure of bulk heterojunction and increase its light conversion efficiency [2-4]. Such a treatment leads to the formation of crystalline regions in an amorphous polymer matrix. This process is accompanied by the shift of light absorption maximum to the lower photon energies due to the increase in the conjugation length in the crystallites. The charge carrier lifetime is usually estimated from photocurrent transients after the excitation by a short light pulse. However, in organic materials this method is inaccurate, because the photocurrent transients depend not only on the decay of charge carrier concentration but also on the mobility relaxation within the broad density of states [42]. To estimate lifetimes from transient absorption techniques is difficult because of the very large dispersion observed leading to power law decays [43].

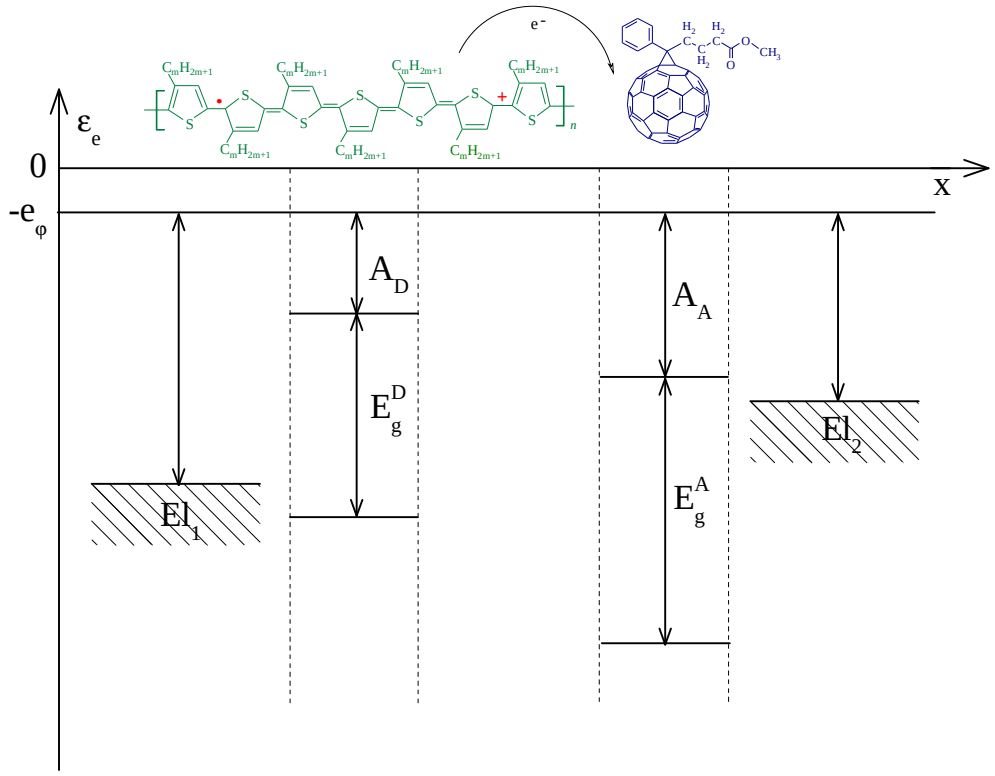

Figure 1. Schematic band diagram of two semiconductors with different electron affinity before making between them bulk heterojunction. The electron donor (A_D) and electron acceptor (A_A) affinities are defined vs. the electron energy in vacuum at the same electrical potential. E_g^D and E_g^A are the bandgap energies of the electron donor and electron acceptor, respectively. In the top, the P3AT and PCBM are schematically shown as electron donor and electron acceptor, respectively. The appearance of a polaron quasi-particle with a spin S = ½ and an elemental positive charge in a P3AT chain is shown as well.

Charge recombination is considered to be predominantly nongeminate process governing effectiveness of polymer/fullerene solar cells [43-47]. Normally, the delay of charge carriers consists of prompt and persistent contributions [47]. The excitation light intensity dependence of a prompt is of bimolecular type and implies mutual annihilation within the created radical pair. The persistent contribution is independent of the excitation intensity and originates from deep traps due to disorder [48]. Bimolecular and quadrimolecular recombinations were shown [17] to be dominant in the P3AT/fullerene composite respectively at lower and higher intensity of the excited light. The time decay of the LEPR intensity was explained by the latter model. It was detected at the temperature increase a crossover from tunneling to activation hopping charge transfer with the activation energy of 0.10 eV. The annihilation of radical pairs in bulk heterojunction of a composite can be described as thermally activated bimolecular process [2, 49]. The existence of long-lived polaron-like excitons with spin S = ½ and effective mass $m_{eff} \approx 300m_e$ [50] apparently complicates the recombination mechanism. The recombination of the long-lived photoinduced polarons in regioregular P3AT consists of temperature independent fast and exponentially temperature dependent slow hyperbolic decay contributions [51]. So, the photoinduction of charge carrier pairs and their

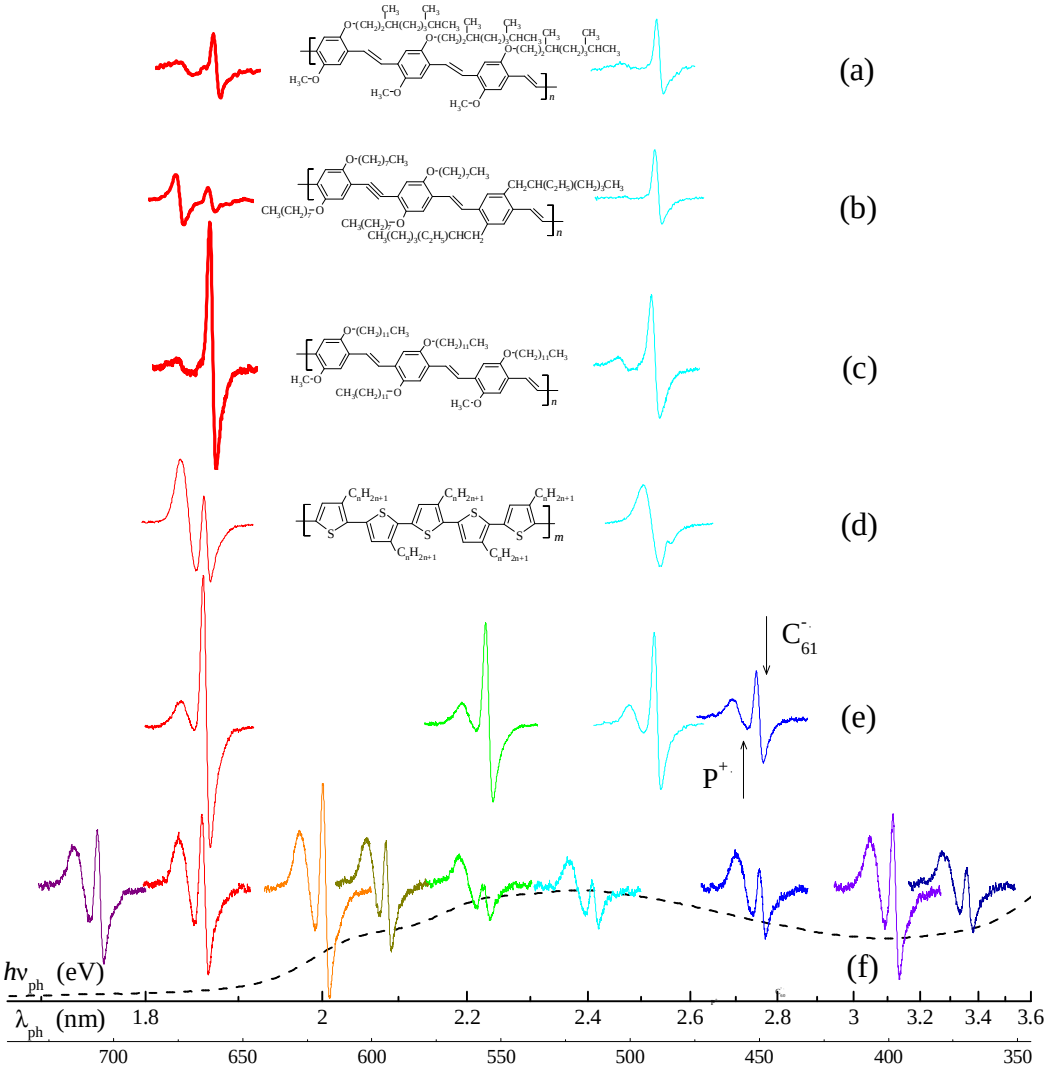

Figure 2. LEPR spectra of radical pairs background photoinduced in bulk heterojunctions of PCBM molecules with macromolecules of poly[2-methoxy-5-(3',7'-dimethyloctyloxy)-1,4-phenylene vinylene] (*a*), poly[1,4-(2,5-dioctyloxyphenylene)ethine-1,4-(2,5-dioctyloxyphenylene)ethane-1,2-diyl-1,4-(2,5-di(2-ethylhexyloxy) phenylene)ethane-1,2-diyl] (*b*), poly[1,4-(2-methoxy-5-dodecyloxyphenylene)ethane-1,2-diyl-1,4-(2,5-didodecyloxyphenylene)ethene-1,2-diyl] (*c*), and of regioregular poly(3-alkylthiophenes-2,5-diyl) (P3AT), poly(3-octylthiophene-2,5-diyl) (n = 8, $P3AT_8$) (*d*), poly(3-dodecylthiophene-2,5-diyl) (n = 12, $P3AT_{12}$) (*e*), and poly(3-hexylthiophene-2,5-diyl) (n = 6, $P3AT_6$) (*f*) by light with different photon energy $h\nu_{ph}$ (linewidth λ_{ph}) at 77 K. The optical absorption spectrum of the $P3AT_6$/PCBM composite is shown by dashed line. The positions of polaron $P^{+\cdot}$ and methanofullerene anion radical $mC_{61}^{-\bullet}$ are shown as well.

recombination are the most interesting points. However, they are not yet sufficiently understood in detail and there is no generally applicable model available.

Except for intermolecular charge transport, charge transfer by polaron along (Q1D) and between (Q3D) polymer chains and uniaxial pseudorotation of fullerene globuls are also

realized in such polymer/fullerene system. These molecular and electronic processes should undoubtedly correlate in such systems. Understanding the basic physics underlying the electron relaxation and dynamic behavior of fullerene-modified organic polymers is essential for the optimization of devices based on these materials.

Charge in initial conjugated polymers is transferred by nonlinear excitations, polarons $P^{+\bullet}$ characterized by spin S = ½ and high mobility along a conjugated polymer backbone [52]. Their magnetic, relaxation and dynamic properties were studied by conventional [53, 54] and high-frequency [55-57] electron paramagnetic resonance (EPR) methods. Photoinduced charge transfer is accompanied by the formation of radical pairs $P^{+\bullet} - C_{60}^{-\bullet}$ of paramagnetic centers each with spin S = ½. This accounts for the widely use of the light-induced EPR (LEPR) as direct method for investigation of fullerene-modified conjugated polymers [58, 59], P3AT among them [17-26]. LEPR measurements revealed the existence of two radicals with different line shapes, magnetic-resonance parameters and saturation properties. The method allowed to detect two photoinduced charge carriers with a prompt and a persistent live in polymer/fullerene system [48].

Let consider how the LEPR method can be used for the more detailed study of magnetic, relaxation and dynamic parameters of paramagnetic centers photoinduced in bulk heterojunctions formed by fullerene molecules embedded into different conjugated polymer matrixes.

We shown earlier [39, 40] that among soluble fullerene derivatives with different side alkyl substitutes [6,6]-phenyl-C_{61}-butanoic acid methyl ester (PCBM or methanofullerene $m$$C_{61}$) is appeared to be more suitable electron acceptor in plastic solar cells. It was found [60] that the mobility and stability of charge carriers is higher considerably in bulk heterojunction formed by the poly(3-hexylthiophene-2,5-diyl) ($P3AT_6$ with n = 6) chains with PCBM molecules as compared with, e.g., poly[2-methoxy-5-(3',7'-dimethyloctyloxy)-1,4-phenylene vinylene] (MDMO-PPV) with embedded PCBM (see Figs. 1 and 2). Much longer charge carrier lifetime achieved in the $P3AT_6$/PCBM film is stipulated by a higher carriers' concentration and their reduced recombination rate. It was explained by better structural order in the presence of interface dipoles provoking the creation of a potential barrier for carrier recombination in this composite. The specific nanomorphology of P3AT/PCBM blends could result in screened Coulomb potential between the radical pairs photoexcited in their bulk heterojunctions and facilitate their splitting into noninteracting charge carriers with a reduced probability of further annihilation. This implies that much longer carrier lifetimes can be achieved at the same concentrations which finally results in higher photocurrent and larger power-conversion efficiency of such solar cells. This predestined the use in our study presented in this Chapter of mainly $P3AT_6$, poly(3-octylthiophene-2,5-diyl) ($P3AT_8$ with n = 8), poly(3-dodecylthiophene-2,5-diyl) ($P3AT_{12}$ with n = 12) as electron donor and PCBM as electron acceptor (Figs. 1 and 2). For the comparison, the respective LEPR study of charge carriers photoinduced in a bulk heterojunctions formed by PCBM with the chains of MDMO-PPV, poly**[**1,4-(2,5-dioctyloxyphenylene)ethine-1,4-(2,5-dioctyloxyphenylene)ethane-1, 2-diyl-1,4-(2,5-di(2-ethylhexyloxy) phenylene)ethane-1,2-diyl] (DE69), and poly[1,4-(2-methoxy-5-dodecyloxyphenylene)ethane -1,2-diyl-1,4 -(2,5 -didodecyloxyphenylene)ethene-1,2-diyl]

(DE107)* (see Figure 2) are considered as well. HOMO and LUMO energetic levels of PCBM were determined cyclic voltammetrically [61] to be equal to -6.1 eV and -3.75 eV, respectively. Energetic data of some conjugated polymers are summarized in Table 1. The optical absorption maximum $h\nu_{max}$ correlates with the energy of π-π* interband transition indicating an increase in planarity of P3AT with the lengthening of backbone alkyl chains [62]. This is due to the fact that longer side groups restrict the number of possible conformations and that two adjacent thiophene rings can form by rotating around their shared C-C bond.

Table 1. The HOMO, LUMO energetic levels, band-gap energy, determined by cyclic voltammetrically (E_g^{CV}) and optically (E_g^{opt}), and absorption maximum $h\nu_{max}$ (all in eV) of some conjugated polymers [20, 61, 63, 64].

Polymer	HOMO	LUMO	E_g^{CV}	E_g^{opt}	$h\nu_{max}$
MDMO-PPV	-5.31	-2.83	2.48	2.12	2.48
DE69	-5.46	-3.56		1.90	2.24
$P3AT_6$	-5.20	-3.53	1.67	1.92	2.48
$P3AT_8$	-5.25	-3.55	1.70	1.92	2.42
$P3AT_{12}$	-5.29	-3.55	1.74	1.93	2.41

2. MAGNETIC RESONANCE PARAMETERS OF RADICAL PAIRS

2.1. Line Shape and *g*-factor

Detached conjugated polymers and methonofullerene are characterized by the absence of both "dark" and photoinduced LEPR signals in the whole temperature range. A dramatic enhancement in the LEPR is observed when mixing both substances together. As the polymer/fullerene composite is irradiated by visible light directly in a cavity of the EPR spectrometer, two overlapping LEPR lines appear at $T \leq 200$ K. Subsequent LEPR measurement cycles of heating up to room temperature, cooling down to $T \leq 200$ K, illumination with light, switching light off, and heating up again yield identical results. Figure 2 shows the LEPR spectra of the polaron $P^{+\bullet}$ and methanofullerene $mC_{60}^{-\bullet}$ radical pairs background photoinduced at 77 K in bulk heterojunctions formed by PCBM molecules with different macromolecules as function of the photon energy $h\nu_{ph}$ (linewidth λ_{ph}). The optical

* Copolymers DE69 and DE107 were synthesized in the Institute for Organic Chemistry and Macromolecular Chemistry, University of Jena. Fullerene derivative PCBM was synthesized in the Zernike Institute for Advanced Materials, University of Groningen.

Table 2. The terms ΔB_{pp}^{i} of linewidth (all in Gauss) LEPR spectra of polarons and fullerene anion radicals used for simulation of the LEPR spectra of the P3AT$_{12}$/PCBM composite obtained at different laser photon energy $h\nu_{ph}$ (in eV) and 77 K.

		$h\nu_{ph}$		
Linewidth	Radical	1.88	2.22	2.75
ΔB_{pp}^{X}	$P^{+\bullet}$	1.98	2.09	2.21
	$mC_{61}^{-\bullet}$	1.04	0.97	1.08
ΔB_{pp}^{Y}	$P^{+\bullet}$	1.98	2.10	2.21
	$mC_{61}^{-\bullet}$	1.12	1.05	1.16
ΔB_{pp}^{Z}	$P^{+\bullet}$	2.58	2.53	2.61
	$mC_{61}^{-\bullet}$	1.02	1.09	1.15
ΔB_{pp}^{iso}	$P^{+\bullet}$	2.18	2.24	2.34
	$mC_{61}^{-\bullet}$	1.06	1.04	1.13

absorption spectrum of the P3AT$_6$/PCBM composite is presented in the same figure.

Each sum spectrum presented in Figure 2 is attributed to radical pairs $P^{+\bullet} - mC_{61}^{-\bullet}$ of positively charged polarons $P^{+\bullet}$ occupying approximately five monomer units and diffusing along polymer chains [51] with isotropic (effective) g_{iso} = 2.0023 and negatively charged anion radicals $mC_{61}^{-\bullet}$ with effective g_{iso} = 2.0001 librating near own main molecular axis. Generally, the deviation Δg of the g-factor of polarons in such conjugated π-electron systems from the free-electron g-factor, g_e = 2.00232, is due to noncompensated orbital momentum, which induces an additional magnetic field during the consequence of σ → π → σ* excitations [65]. In this case this parameter depends on the spin-orbit coupling λ and the energy differences between the σ and π levels, $\Delta E_{\sigma\pi}$, and between the π and σ* levels, $\Delta E_{\pi\sigma^*}$:

$$\Delta g = -\frac{\lambda}{3}\left(\Delta E_{\sigma\pi}^{-1} - \Delta E_{\pi\sigma^*}^{-1}\right). \quad (1)$$

The orbital moment due to a direct π-π* excitation is negligible and shows up on the neighboring C atoms only. On the other hand, the g-factor anisotropy is induced by additional fields along the x and y directions within the plane of the σ skeleton and not along the perpendicular z direction. Indeed, our high-field/frequency EPR study of paramagnetic centers in P3AT$_8$ shown [66, 67] that the interaction of an unpaired electron delocalized on a polaron with sulphur heteroatoms involved in the polymer backbone leads to rhombic anisotropy of its g-factor, g_{xx} = 2.00409, g_{yy} = 2.00332 and g_{zz} = 2.00235. The effective g_{iso} of

anion radicals $mC_{61}^{-\bullet}$ is typical of other fullerene anion radicals [68]. De Ceuster et al. shown [69] that the spin density in $mC_{61}^{-\bullet}$ anion radical embedded into organic polymer matrix is also characterized by rhombic symmetry and, therefore, anisotropic g-factor, g_{xx} = 2.00031, g_{yy} = 2.00011 and g_{zz} = 1.99821. As in the case of the initial C_{60} molecule [70-73], the deviation of the g-factor of the PCBM anion radical from g_e is due to the fact that the orbital angular moment is not completely quenched. Due to the dynamical Jahn-Teller effect accompanying the structural molecular deformation, the isotropic nature of the icosahedral C_{60} globule is distorted after the formation of the $C_{60}^{-\bullet}$ anion radical, resulting in its axial or even lower symmetry [74]. This is also realized in the case of fullerene derivative radicals [69], whose high symmetry is lowered by the bond to the phenyl side chain prior to electron trapping. An asymmetrical distribution of spin density in both the polaron and fullerene anion radical leads also to a tensorial character of their linewidth [66, 67, 69]. This should be taken into account in precise calculation of an effective LEPR spectrum of a polymer matrix with embedded fullerenes. The main values and traces of the $\boldsymbol{g}$-tensors of the $P^{+\bullet}$ and $mC_{61}^{-\bullet}$ radicals determined by that means, e.g., for $P3AT_{12}$/PCBM composite, are respectively g_{xx} = 2.0026, g_{yy} = 2.0017, g_{zz} = 2.0006, $\langle g \rangle$ = 2.0016 and g_{xx} = 2.0003, g_{yy} = 2.0001, g_{zz} = 1.9986, $\langle g \rangle$ = 1.9996. The respective linewidth terms used for the fitting of this LEPR spectrum are presented in Table 2.

2.2. Paramagnetic Susceptibility

Normally, the spins photoinduced in close proximity in ion-radical pairs should interact with own nearest counterions through exchange or dipole-dipole interaction. Since these interactions do not registered in the LEPR spectra, one can conclude that the mobile polarons on the conjugated polymer backbone are moving away from fullerene anions faster than 10^{-9} s. That is a reason why both charge carriers excited in polymer/fullerene composite are characterized by a considerable long lifetime and can be registered separately. Such LEPR spectra should reflect different factors effecting bimolecular annihilation of charge carriers in bulk heterojunction. If one include Coulomb interactions in this model, these should affect the activation energy E_a for either detrapping or thermally assisted tunneling by an amount $U_c = e^2/4\pi\varepsilon\varepsilon_0 r$, where e is the elemental charge, ε is the dielectric constant, and r is the charge pair separation. U_c varies from around 0.4 eV for charges separated by one lattice unit down to 0.02 eV or less for a more distinct charge separation. Therefore, both the photoinduced polaron and anion radical should be considered as noninteracting, which is the cause of their long life.

Integrated LEPR signal of a polymer/fullerene composite shows at 77 K two peaks with comparable areas, indicating that both radicals have equal amounts of spins (Figure 3a). In other words, the shape of the appropriate LEPR spectrum must be independent of the number and energy of photons absorbed by polymer/fullerene compounds with close structure and composition. Besides, the total number of spin charge carriers photoinduced in a polymer/fullerene composite and, therefore, its quantum efficiency should follow its absorption spectrum. However, it is rather far from this conception for the polymer matrix presented in Figure 2. There are different factors leading to such discrepancy, e.g., a different ordering of the composites used, photoinitiation not only mobile but also pinned charge

carriers or/and a possible collapse of polaron couples into spinless bipolarons. It was shown [23, 24, 75] that a variation of irradiation photon energy $h\nu_{ph}$ can also change P3AT/PCBM LEPR spectrum. Indeed, Figure 3a demonstrates that the increase in the $h\nu_{ph}$ value leads to the change in relative concentrations of polarons $P^{+\bullet}$ and fullerene anion radicals $mC_{61}^{-\bullet}$ with extremas at $h\nu_{ph} \approx 2.1$ eV for the $P3AT_{12}$/PCBM composite and at $h\nu_{ph} \approx 2.0$ and 3.1 eV for the $P3AT_6$/PCBM composite. On the other hand, these charge carriers photoinduced in the $P3AT_{12}$/PCBM composite are characterized by respective monotonic and extremal (at $h\nu_{ph} \approx$ 2.3 eV) dependences. This means that the spinless charge carriers formed at irradiation of the P3HT/PCBM composite by photons with $h\nu_{ph}$ = 2.1–2.5 eV should, probably, prevail over polarons. The finite depth of illumination penetration into the samples bulk should also affect their LEPR line shape. Indeed, Figure 2 shows that the intensity and shape of the radical pair LEPR spectrum do not correlate with the light penetration into the sample bulk. Such effect can probably be interpreted in terms of cooperative light penetration into sample bulk and collapse of polaron pairs photoinduced on its surface into diamagnetic bipolarons.

The nature and dynamics of charge carriers in radical pairs can also contribute to their effective LEPR spectrum. Figure 3b shows also how changes paramagnetic susceptibility χ of charge carriers photoinduced at background irradiated in different P3AT/PCBM composites at their heating. One can notice two evident effects from the data presented. The first of them is that the effective number of polarons changes slightly with the temperature, whereas the concentration of fullerene anion radicals dramatically decreases with the composite heating. The second one is the deviation of the spin concentrations ratio χ_P/χ_{C61} from the unit at $T > 77$ K. Such effect can be interpreted as following.

Let a polaron possessing a positive charge multihops along a polymer chain from one initial site i to other available site j close to a position occupied by a negatively charged fullerene globule. Charge hops more easily between fullerenes than from polaron and fullerene, and an effective charge recombination is still limited by the transport of polarons towards fullerene molecules. The recombination is mainly stipulates by sequential charge transfer by polaron along a polymer chain and its transfer from polymer chain to a site occupied by a fullerene. Polaronic dynamics in undoped and slightly doped conjugated polymers is highly anisotropic [56]. [66, 66, 67]Therefore, the probability of a charge transfer along a polymer chain exceeds considerably that of its transfer between polymer macromolecules.

According to the tunneling model [76], positive charge on a polaron can tunnel from this carrier toward a fullerene and recombine with its negative charge during the time

$$\tau(R_{ij}^{|}) = \frac{\ln X}{\nu_{pn}} \exp\left(\frac{2R_{ij}^{|}}{a_0}\right), \qquad (2)$$

where $R_{ij}^{|}$ is the spatial separation of sites i and j, a_0 is the effective localization (Bohr) radius, X a random number between 0 and 1, and ν_{pn} is the attempt to jump frequency for positive charge tunneling from polymer chain to fullerene. The charge

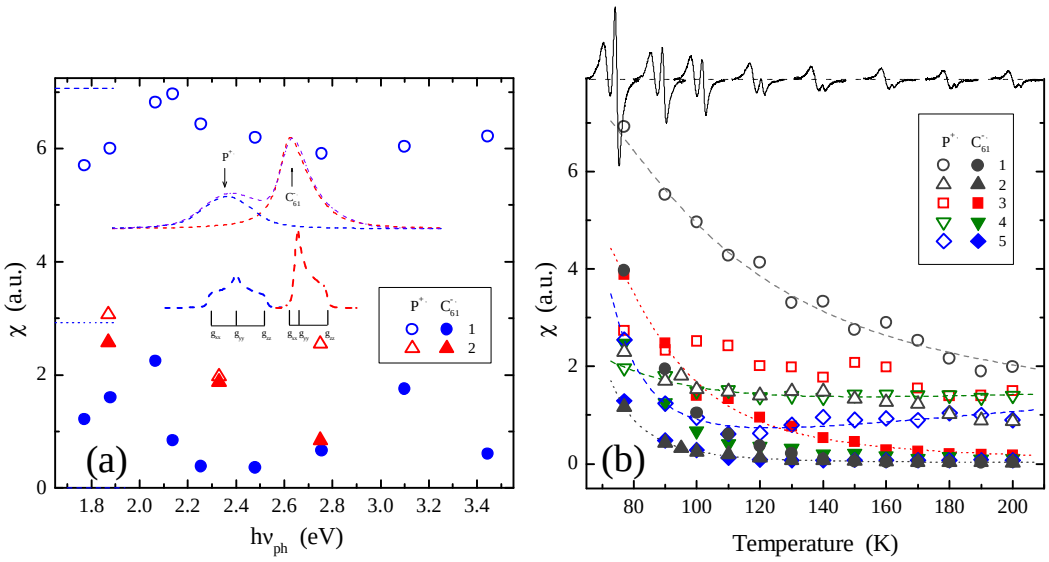

Figure 3. (*a*) Paramagnetic susceptibility χ of the polarons $P^{+\bullet}$ (open points) and methanofullerene anion radicals $mC_{60}^{-\bullet}$ (filled points) photoinduced at 77 K in the $P3AT_6$/PCBM (*1*) and $P3AT_{12}$/PCBM (*2*) composites as function of the photon energy $h\nu_{ph}$. Spin susceptibility determined for these charge carriers initiated by white light in the $P3AT_6$/PCBM sample are shown by the dashed and dotted line sections, respectively. In the insert are shown integral contributions of both charge carriers characterizing with anisotropic g_{ii}-factors to the sum LEPR spectrum of a composite. (*b*) Temperature dependence of the χ parameter determined for the $P^{+\bullet}$ (open points) and $mC_{61}^{-\bullet}$ (filled points) charge carriers photoinduced by white light in the initial (*1*) and annealed (*2*) $P3AT_6$/PCBM composites as well as by photons with energy 1.88 eV (*3*), 2.22 eV (*4*), and 2.75 eV (*5*) in the $P3AT_{12}$/PCBM composite. Some dependences calculated from Eq.(5) with different ΔE_{ij} are shown by dashed lines as an example. In the top are shown how changes with the temperature a typical LEPR spectrum of radical pairs steady-state photoinduced in a polymer/fulleren composite.

can also be transferred by the polaron thermally assisted multistep tunneling through energy barrier $\Delta E_{ij} = E_j - E_i$ with the time [76]

$$\tau(R_{ij}, \Delta E_{ij}) = \frac{\ln X}{\nu_{pp}} \exp\left(\frac{2R_{ij}}{a_0}\right) \exp\left(\frac{\Delta E_{ij}}{k_B T}\right), \qquad (3)$$

where ν_{pp} is the attempt frequency for a hole tunneling between the polymer chains, k_B is a Boltzmann constant, and T is the temperature. The values in the couples ν_{pn}, ν_{pp} and $R_{ij}^{|}$, R_{ij} may be different due, for instance, to the different electronic orbitals. The localization radius a_0 for a negative charged carrier in a polymer/fullerene composite should be on the order of the radius of the PCBM globule. The distance R_{ij} should depend, e.g., on the length of a side alkyl chain substitute of regioregular P3AT [77]. Polaron stabilized in conjugated polymers is normally distributed over five monomer units [51, 78].

The decay of polaron charge carriers in regioregular P3AT consists of temperature independent fast and exponentially temperature dependent slow contributions [51].

Additionally to the above mentioned tunneling and activation processes, there should be one more contribution of polarons to effective spin susceptibility. The matter is that, undoubtedly, positive charge on polaron is not required to be recombined with the first negative charge but with charge on the subsequent fullerene. Thus, the probability of charge annihilation can differ from the unit. Besides, the polaronic quasi-particle is characterized by 1D mobility. Such fundamental properties of this specific charge carrier require considering also the contribution to its paramagnetic susceptibility due to exchange interaction of both types of paramagnetic centers. Positively charged polaron 1D hopping from site *i* to site *j* with frequency ω_{hop} may collide with a fullerene anion radical situated near polymer matrix. Whereas the polaron is mobile, the fullerene globe can be considered as translative fixed, however, pseudorotating near own main molecular axis. In this case the probability *p* of spin flip-flop during a collision should depend on the amplitude of exchange and ω_{hop} value as [79]

$$p = \frac{1}{2} \cdot \frac{\alpha^2}{1+\alpha^2}, \tag{4}$$

where $\alpha = 3\pi J/\mathbf{h}\omega_{hop}$, $\mathbf{h} = h/2\pi$ is the Plank constant and *J* is the constant of exchange interaction of the spins in a radical pair. Either weak or strong exchange limits can be realized in illuminated polymer/fullerene composite. In the case of weak or strong exchange, the increase in ω_{hop} may result in the decrease or increase in exchange frequency, respectively. If the ratio $J/\mathbf{h}$ exceeds the frequency of collision of both types of spins, the condition of strong interaction is realized in the system leading to a direct relation of spin-spin interaction and polaron diffusion frequencies, so then $\lim(p) = 1/2$. In the opposite case $\lim(p) = 9/2\,(\pi/\mathbf{h})^2\,(J/\omega_{hop})^2$. It is evident that the longer both the above tunneling times or/and the lesser the probability *p*, the smaller the number of ion-radical pairs that have a possibility to recombine and, therefore, the higher spin susceptibility should be obtained. A combination of the above equations takes, therefore, the general form of this main parameter for polarons in polymer/fullerene composite as

Table 3. The ΔE_{ij} and E_a values (all in eV) determined from Eqs.(5) and (6), respectively, for radical pairs photoinduced by white light in the initial and annealed $P3AT_6$/PCBM composite as well as by laser beam with different photon energy $h\nu_{ph}$ in the $P3AT_{12}$/PCBM system.

	Composite									
	$P3AT_6$/PCBM				$P3AT_{12}$/PCBM					
	Initial		Annealed		$h\nu_{ph}$= 1.88 eV		$h\nu_{ph}$= 2.22 eV		$h\nu_{ph}$= 2.75 eV	
Radical Parameter	$P^{+\bullet}$	$mC_{61}^{-\bullet}$	$P^{+\bullet}$	$mC_{61}^{-\bullet}$	$P^{+\bullet}$	$mC_{61}^{-\bullet}$	$P^{+\bullet}$	$mC_{61}^{-\bullet}$	$P^{+\bullet}$	$mC_{61}^{-\bullet}$
ΔE_{ij}	0.012	0.042	0.008	0.045	0.006	0.028	0.031	0.036	0.084	0.051
E_a	0.015		0.017		0.041		0.003		0.019	

$$\chi_p = \chi_{pn} + \chi_P^0 \frac{\mathbf{h}}{J}\left(\alpha + \frac{1}{\alpha}\right). \quad (5)$$

Assuming the above introduced activation character for polaron multistep hopping with the frequency $\omega_{hop} = \omega_{hop}^0 \exp(-\Delta E_{ij}/k_B T)$ and the absence of dipole-dipole interaction between fullerene anion radicals, one can determine ΔE_{ij} (see Table 3) and J parameters from individual temperature dependences of paramagnetic susceptibility.

It is seen from Figure 3b that the dependences presented are fitted well by Eq.(5) with the ΔE_{ij} values summarized in Table 3. The Figure shows that the polaron charge carriers photoinduced in different P3AT/PCBM composites are characterized by a weaker $\chi(T)$ dependence as compared with that of fullerene anion radicals. ΔE_{ij} obtained for polarons photoinduced by white light in the $P3AT_6$/PCBM composite slightly decreases after its heat treatment, whereas this value determined for fullerene anion radicals changes remarkably smaller (Table 3). However, this parameter obtained for both type of charge carriers in the $P3AT_{12}$/PCBM composite seems to increases monotonically with the growing of the photon energy $h\nu_{ph}$. One can conclude that polaronic dynamics in the $P3AT_6$/PCBM composite is activated at comparatively smaller ΔE_{ij} then in the $P3AT_{12}$/PCBM one. This occurs due, probably, to the more structural inhomogeniety and larger number traps in the latter polymer matrix. The J constant was analyzed to change slightly within 0.2 – 0.35 eV. This value sufficiently exceed an appropriate constant of spin collision of nitroxide radicals with paramagnetic ions in liquids, $J \leq 0.01$ eV [80], however, this lie near $J \approx 0.36$ eV we obtained for interaction of polarons with the oxygen molecules in polyaniline highly doped by *p*-toluenesulfonic acid [81, 82].

2.3. Linewidth

Effective (isotropic) peak-to-peak linewidths $\Delta B_{pp}^{(0)}$ obtained for the $P^{+\bullet}$ and $mC_{61}^{-\bullet}$ radicals in the absence of their microwave saturation are presented in Figure 4 as a function of photon energy and temperature. It is seen from Figure 4a that this parameter determined for both charge carriers changes nonmonotonically with photon energy $h\nu_{ph}$ with the extremas near 2.0 and 3.1 eV. The first extreme lies near the band-gap energy E_g^{opt} of the polymer matrix (Table 1), whereas the second one can probably be attributed to inhomogeneous distribution of domains with different ordering (and, hence, band-gap energies) in the polymer/fullerene composite. Analyzing the temperature data presented in Figure 4b one can notice that the linewidth of polarons in the $P3AT_{12}$/PCBM composite changes monotonically with its heating, whereas fullerene radicals demonstrate more complex $\Delta B_{pp}^{(0)}(T,\nu_{ph})$ dependence. Polarons stabilized in the $P3AT_6$/PCBM composite also demonstrate extremal temperature dependence of linewidth. Extrapolation to room temperature gives 1.8 and 2.9 G for $P^{+\bullet}$ photoinduced respectively in $P3AT_6$ and $P3AT_{12}$ matrices, which lie near $\Delta B_{pp}^{(0)}$ = 1.3 – 1.8 G obtained for polarons stabilized in different P3AT [53, 54]. However, this value is considerably less then that determined for undoped polythiophene [53, 54, 83] that is evidence of weaker spin interaction in the P3AT lattice. LEPR linewidth should reflect

different processes occurring in a P3AT/PCBM composite. One of them is the association of mobile polarons with the countercharges. Another process realizing in the system is dipole-dipole interaction between mobile and trapped polarons and fullerenes that broadens the line by $\Delta B_{dd} = \mu_B / R_0^3 = 4/3\pi\mu_B n_P$, where μ_B is the Bohr magneton, R_0 is the distance between dipoles proportional to the polaron concentration n_P on the polymer chain. Extrapolating temperature dependences to the lower temperature limit, *i.e.* when the temperature tends to zero, one obtains $\Delta B_{pp}^{(0)} \approx 1.4 – 1.7$ G for polarons and $\Delta B_{pp}^{(0)} \approx 0.7 – 0.8$ G for fullerene anion radicals and, therefore, $R_0 \approx 2.6 – 2.9$ nm for a distance between dipoles in the P3AT/PCBM composite.

Assuming exchange and activation interaction of the fullerene anion radical quasifixed near a polymer chain with polaron hopping along the chain with the rate ω_{hop}, the dependences presented in Figure 4b can also be described in terms of the above mentioned Houze-Nechtschein approach [79]. According to this theory, the collision of both types of spins should additionally broaden the absorption LEPR line by the value [79]

$$\delta(\Delta\omega) = p\omega_{hop}C = \frac{1}{2}\omega_{hop}C\left(\frac{\alpha^2}{1+\alpha^2}\right), \qquad (6)$$

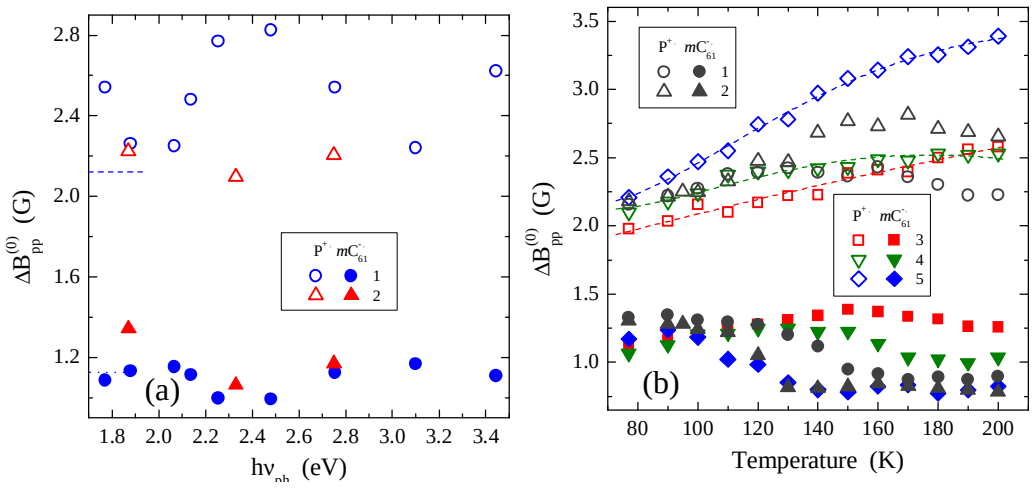

Figure 4. (*a*) A lower limit of the peak-to-peak linewidth $\Delta B_{pp}^{(0)}$ of the polarons $P^{+\bullet}$ (open points) and methanofullerene anion radicals $mC_{61}^{-\bullet}$ (filled points) photoinduced at 77 K in the $P3AT_6$/PCBM (*1*) and $P3AT_{12}$/PCBM (*2*) composites as function of the photon energy $h\nu_{ph}$. Linewidths determined for polarons and fullerene anion radicals initiated by white light in the $P3AT_6$/PCBM sample are shown by the dashed and dotted line sections, respectively. (*b*) Temperature dependence of the linewidth determined for these charge carriers photoinduced by white light in the initial (*1*) and annealed (*2*) $P3AT_6$/PCBM composites as well as by photons with energy 1.88 eV (*3*), 2.22 eV (*4*), and 2.75 eV (*5*) in the $P3AT_{12}$/PCBM composite. Some dependences calculated from Eq.(6) with different E_a presented in Table 3 are also shown as an example.

where p is probability described by Eq.(4), $\omega_{hop} = \omega^0_{hop} \exp(-E_a/k_B T)$, C is the number of paramagnetic centers per each polymer unit, and E_a is the activation energy.

The dependences calculated from Eq.(6) with E_a presented in Table 3 are also shown in Figure 4b. The analysis of the data presented allows the conclusion that the energy required for activation of polaron diffusion in the $P3AT_6$/PCBM composite changes only slightly at its heat treatment. However, this parameter obtained for the $P3AT_{12}$/PCBM composite decreases nonmonotonically with the increase in the energy of the photons initiating charge separation (see Table 3).

It is seen that the main magnetic resonance parameters of charge carriers are governed by the energy of light photons. This can be realized either at the formation of spin pairs with different properties in homogeneous composite fragments or at the excitation of identical charge carriers in heterogeneous domains of a composite. Different spin pairs can be photoinduced as a result of photon-initiated appearance of traps with different depth in polymer matrix. However, the difference in the parameters of paramagnetic centers revealed seems to be rather a result of their interaction with their own microenvironment in domains inhomogeneously distributed in the polymer/fullerene composite. Different orderings of these domains can be a reason for their different band gaps and, hence, their sensitivities to photons with defined but different energies. This can give rise to a variation in an interaction of paramagnetic centers with a lattice and other spins.

3. RECOMBINATION OF CHARGE CARRIERS

In solar cells, both charges diffusing to the opposite electrodes must reach them prior to recombination. If these chargers after their transfer are still bound by the Coulomb potential, which is typical for the described here compounds with low-mobile charge carriers, they cannot escape from each other's attraction and will finally recombine. When the carrier dissipation distance is longer than the Coulomb radius, the excitons photoinduced can be split into positive and negative charge carriers. To fulfill this condition, the Coulomb field must be shielded or charge carrier hopping distance must exceed the Coulomb radius. In this case charges are transferred to the electrodes either by the diffusion of appropriate carriers or by the drift induced by the electric field. In order to excite a radical pair by each photon, charge carrier transit time t_{tr} should be shorter considerably than the lifetime of a radical pair τ, i.e., $t_{tr} << \tau$. The former value is determined by charge carrier mobility μ, sample thickness d, and electric field E inside the film, $t_{tr} = d/\mu E$. If photocurrent is governed by the carrier drift in the applied electric field, the drift distance $l_{dr} = \mu\tau E$. If this current is governed by carrier diffusion, the diffusion distance $l_{diff} = (D\tau)^{1/2} = (\mu\tau k_B T/e)^{1/2}$, where D is the diffusion coefficient, and e is the elemental electron charge. Thus, the $\mu\tau$ product governs the average distance passed by the charge carrier before recombination and, therefore, is an important parameter determining whether the efficiency of solar cells is limited by charge transport and recombination.

If one switches off excited light illumination of the polymer/fullerene system, the concentration of spin pairs excited in its bulk heterojunction starts to decrease. Figure 5 shows typical decay curves of both spin carriers excited in the $P3AT_6$/PCBM composite at T = 77 K. There can be different progress for a radical pair after the illumination interruption,

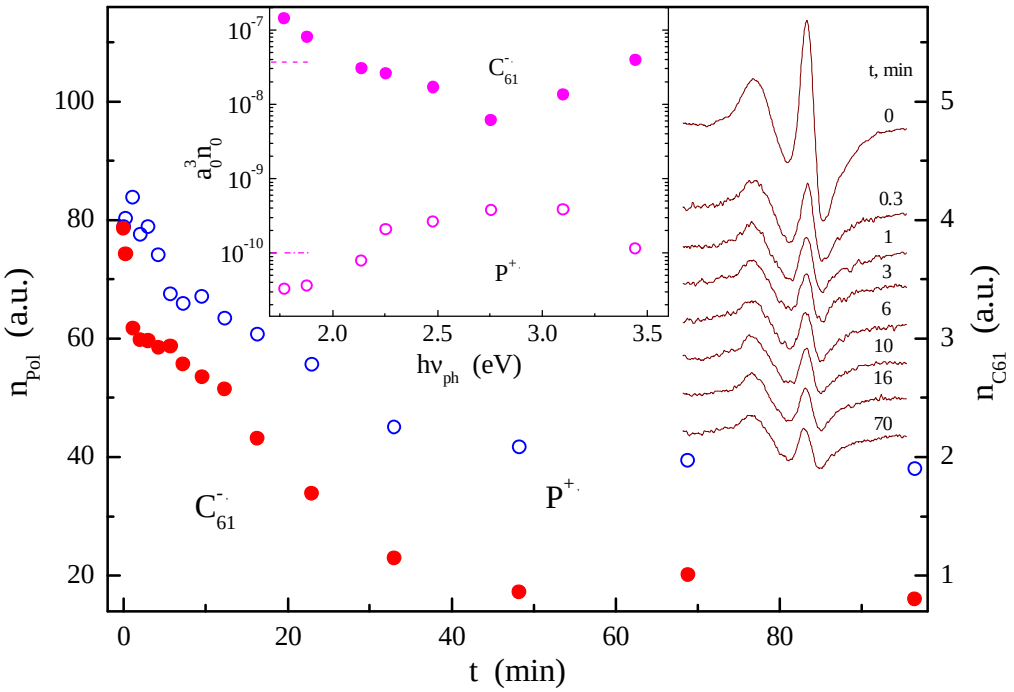

Figure 5. Typical time dependence of the concentration of the polarons $P^{+\bullet}$ (open points) and methanofullerene anion radicals $mC_{61}^{-\bullet}$ (filled points) photoinduced in polymer/fullerene composite after light irradiation blackout. In the right insert it is shown how changes typical LEPR spectrum of a composite polymer/fullerene with the time *t*, whereas the central insert demonstrates the change of the $a_0^3 n_0$ term in Eq.(9) of these charge carriers photoinduced in the $P3AT_6$/PCBM composite on the photon energy $h\nu_{ph}$.

instantaneous collapse of the radical pairs or their splitting into noninteracting charge carriers due to polaron diffusion away.

The nearest-neighbor distance R_{ij} [see Eq.(2)] of spin pair with the tipical radiative lifetime τ_0 changes with time *t* as

$$R_{ij}(t) = \frac{a_0}{2} \ln\left(\frac{t}{\tau_0}\right). \tag{7}$$

Assuming that photoexcitation is turned off at some initial time $t_0 = 0$ at a charge carrier concentration n_0 and taking into account a time period of geminate recombination $t_1 - t_0$, one can write for concentration of charge carriers

$$n(R_{ij}) = \frac{n}{1 + \frac{4\pi}{3} n_1 \left(R_{ij}^3 - R_1^3\right)}, \tag{8}$$

where R_{ij} is specified by Eq.(7), $R_1 = R_{ij}(t_1)$ describes the distance between the nearest-neighbor charge carriers at time t_1 after which solely nongeminate recombination is assumed,

and n_1 is the charge carrier concentration at time t_1. It follows from Eq.(9) that the time dependence of residual carrier concentration does not follow a simple exponential decay but shows a more logarithmic time behavior. After very long times, i.e., at large R_{ij}, one obtains $n(R_{ij}) = [(4\pi/3) R_{ij}^3]^{-1}$ which is independent of the initial carrier density n_1 and also n_0. It follows from Eq.(2) that photoexcited charge carriers have comparable long lifetimes which are solely ascribed to the large distances between the remaining trapped charge carriers. The excited carrier concentration n_1 follows directly from LEPR measurements, whereas the a_0 and τ_0 values can be guessed in a physically reasonable range. Finally, the concentration of spin pairs should follow the relation [84]

$$\frac{n(t)}{n_0} = \frac{\frac{n_1}{n_0}}{1+\left(\frac{n_1}{n_0}\right)\frac{\pi}{6}a_0^3 n_0\left[\ln^3\left(\frac{t}{\tau_0}\right)-\ln^3\left(\frac{t_1}{\tau_0}\right)\right]}. \tag{9}$$

The analysis shown that depending on the photon energy $h\nu_{ph}$ the spin concentration initially photoexcited at $t = 0$ is governed by some factors. The $a_0^3 n_0$ terms of Eq.(9) determined for both photoexcited paramagnetic centers are also shown in the insert in Figure 5 as function of the photon energy $h\nu_{ph}$. As the Figure indicates, these values changes symbatically with $h\nu_{ph}$. It was shown that Eq.(9) fits well the experimental data presented in Figure 5. Therefore, a decay of long-living spin pairs photoinduced in the P3AT/PCBM and analogous composites can successfully be described in the framework of the above model in which the low-temperature recombination rate is particularly strongly dependent on the spatial distance between photoinduced charge carriers. The long lifetimes are solely ascribed to the large spatial distances that build up among the remaining photoinduced charge carriers, which have not recombined at a shorter time.

4. ELECTRON RELAXATION OF RADICAL PAIRS

As the magnetic term B_1 of the steady-state microwave field increases, the linewidth ΔB_{pp} of a LEPR spectrum broadens and its intensity I_L first increases linearly, plateaus starting from some B_1 value and then decrease as it is shown in Figure 6. This occurs due to manifestation of a microwave steady-state saturation effect in the LEPR spectrum of composite. Polaron and fullerene anion radical are noninteracting and, therefore, independent of one another. This stipulated independing of their LEPR signals allowing us to use such effect for separate estimation of their spin-lattice T_1 and spin-spin T_2 relaxation times from relations [85]

$$\Delta B_{pp} = \Delta B_{pp}^{(0)}\sqrt{1+\gamma_e^2 B_1^2 T_1 T_2} \tag{10}$$

and

$$I_L = I_L^{(0)} B_1 \left(1+\gamma_e^2 B_1^2 T_1 T_2\right)^{-3/2}, \tag{11}$$

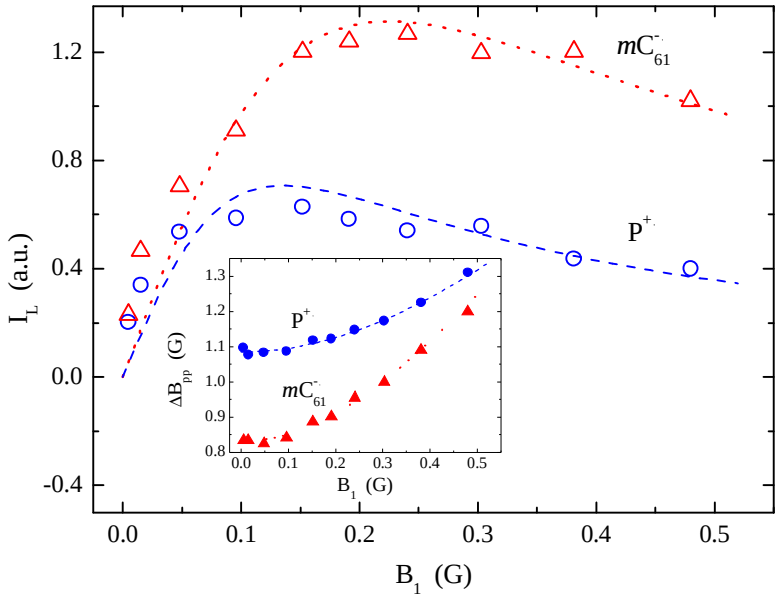

Figure 6. Typical dependences of the intensity I_L and peak-to-peak linewidth (insert) LEPR spectrum of the polarons $P^{+\bullet}$ (open points) and methanofullerene anion radicals $mC_{61}^{-\bullet}$ (filled points) photoinduced in a polymer/fullerene composite on the polarizing microwave field B_1 in a center of the spectrometer cavity. The lines show the dependences calculated from Eqs.(10) and (11) with $T_1 = 2.9\text{x}10^{-6}$ s and $T_2 = 6.1\text{x}10^{-8}$ s (dashed lines), $T_1 = 1.1\text{x}10^{-6}$ s and $T_2 = 7.2\text{x}10^{-8}$ s (dotted lines).

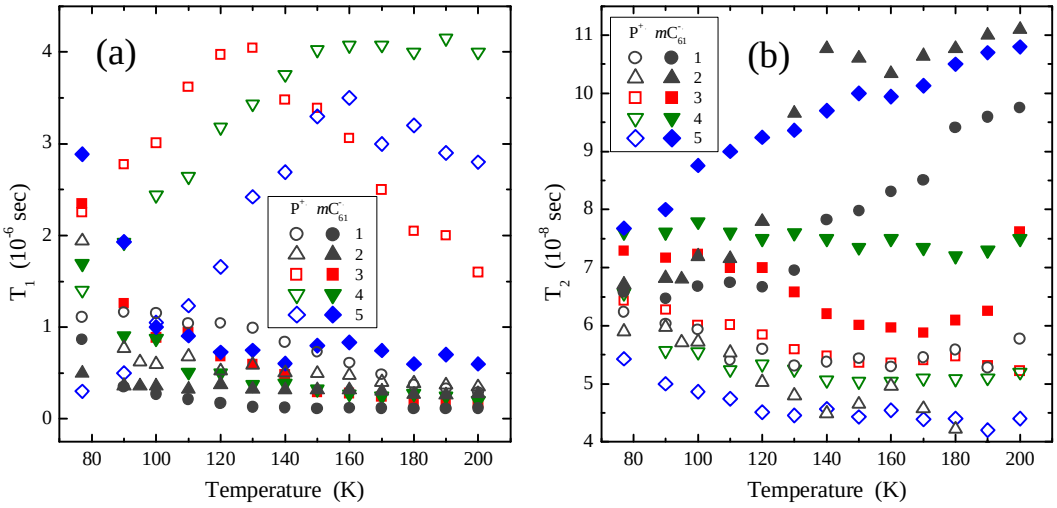

Figure 7. Temperature dependency of the spin-lattice T_1 (*a*) and spin-spin T_2 (*b*) relaxation times determinede from Eqs.(10) and (11) for the polarons $P^{+\bullet}$ (open points) and methanofullerene anion radicals $mC_{61}^{-\bullet}$ (filled points) photoinduced by a white light in the initial (*1*) and annealed (*2*) $P3AT_6$/PCBM composites as well as in the $P3AT_{12}$/PCBM composite by laser with photon energy of 1.88 eV (*3*), 2.22 eV (*4*), and 2.75 eV (*5*).

where $I_L^{(0)}$ is intensity of nonsaturated spectrum, $T_2 = 2/\sqrt{3}\gamma_e \Delta B_{pp}^{(0)}$, and γ_e is the gyromagnetic ratio for electron. The inflection point characteristic for polarons' saturation curve is distinct from that obtained for fullerene anion radicals. This is evidence of different relaxation parameters of these paramagnetic centers and confirms additionally their mutual independence.

The relaxation parameters of polarons and fullerene anion radicals determined using such a method are presented in Figure 7 as function of temperature.

The analysis of the data obtained shows that the electron relaxation of charge carriers photoinduced in the initial P3AT$_6$/PCBM composite changes monotonically with the temperature. The annealing of the composite causes the nonlinearity of the $T_2(T)$ functions of both charge carriers near 140 K as well as the decrease in spin-lattice relaxation time of fullerene radical anions (Figure 7b). The interaction of anion radicals $m\mathrm{C}_{61}^{-\bullet}$ with a polymer matrix in the P3AT$_{12}$/PCBM composite is also characterized by monotonic temperature dependence, whereas the T_1 value of polarons $\mathrm{P}^{+\bullet}$ demonstrates extremal temperature dependence with a critical temperature $T_c \approx 130 - 160$ K. The latter value depends on the photon energy $h\nu_{ph}$ (Figure 7). Spin-spin relaxation of these radicals is accelerated monotonically at the temperature increase. This nearly holds for both the charge carriers except T_2 of methanofullerene anion-radical $m\mathrm{C}_{61}^{-\bullet}$ photoinduced by photons with $h\nu_{ph} = 2.75$ eV (Figure 7). Such peculiarities argue that the mechanism and the rate of electron relaxation depend on the structure and conformation of the initial and fullerene-modified polymer matrices. The data obtained show the effect of the photon energy on relaxation parameters of radical pairs photoinduced in polymer/fullerene composites. This can also be explained by the formation of photoinitiated charge carriers in differently ordered domains with their respective band-gaps.

5. DYNAMICS OF CHARGE CARRIERS

Various spin-aided dynamic processes occur in polymer/fullerene composites: polaron diffusion along and between polymer chains with coefficient D_{1D} and D_{3D}, respectively, pseudorotational diffusion (libration on short angles) of fullerene anion radical near own main molecular axis with coefficient D_{rot}. These processes induce an additional magnetic field in the whereabouts of electron and nuclear spins which, in turn, accelerates electron relaxation in both spin ensembles. As relaxation of the whole spin reservoir in an organic conjugated polymer is defined mainly by a dipole-dipole interaction between electron spins [86], these coefficients can be determined from the following equations [87]:

$$T_1^{-1}(\omega_e) = \langle\omega^2\rangle\left[2J(\omega_e) + 8J(2\omega_e)\right], \tag{12}$$

$$T_2^{-1}(\omega_e) = \langle\omega^2\rangle\left[3J(0) + 5J(\omega_e) + 2J(2\omega_e)\right], \tag{13}$$

where $\langle\omega^2\rangle = 1/10\,\gamma_e^4\mathbf{h}^2 S(S+1)n\Sigma_{ij}$ is the constant of a dipole-dipole interaction for powder, n is a number of polarons per each monomer, Σ_{ij} is the lattice sum for powderlike sample, $J(\omega_e) = (2D_{1D}^{|}\,\omega_e)^{-1/2}$ (at $D_{1D}^{|} >> \omega_e >> D_{3D}$), $J(0)=(2D_{1D}^{|}\,D_{3D})^{-1/2}$ (at $D_{3D} >> \omega_e$) are the spectral density

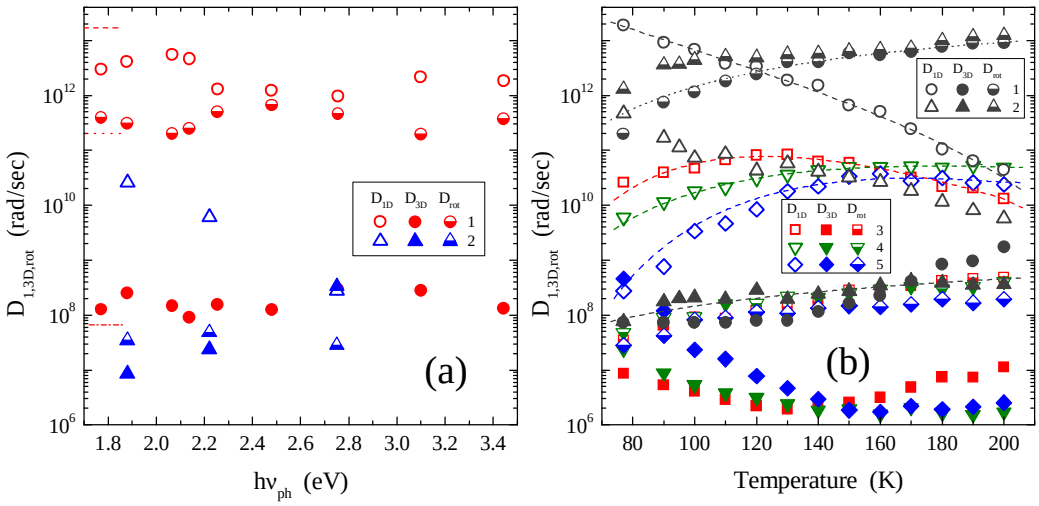

Figure 8. (*a*) The coefficients of polarons $P^{+\bullet}$ hopping along (D_{1D}, open points) and between (D_{3D}, filled points) polymer chains, and the coefficient of pseudorotation of methanofullerene anion radicals $mC_{61}^{-\bullet}$ near main axis (D_{rot}, semi-filled points) photoinduced at 77 K in the $P3AT_6$/PCBM (*1*) and $P3AT_{12}$/PCBM (*2*) composites as function of the photon energy $h\nu_{ph}$ calculated from Eqs.(12) and (13). The coefficients determined for these charge carriers initiated by white light in $P3AT_6$/PCBM sample are shown by the dashed, dash-dotted and dotted line sections, respectively. (*b*) Temperature dependence of the D_{1D}, D_{3D} and D_{rot} parameters determined for these charge carriers photoinduced by white light in the initial (*1*) and annealed (*2*) $P3AT_6$/PCBM composites as well as by laser with photon energy of 1.88 eV (*3*), 2.22 eV (*4*), and 2.75 eV (*5*) in the $P3AT_{12}$/PCBM composite. As an example, in (*b*) are also shown some dependences calculated from Eqs.(14) and (15) with respective lattice phonon E_{ph} and activation barrier E_b energies.

functions for polaron longitudinal diffusion, and $J(\omega_e) = \tau_c/(1+\tau_c^2\omega_e^2)$ is the spectral density function for fullerene pseudorotational diffusion with correlation time τ_c, $D_{1D}^{|}=4D_{1D}/L^2$, ω_e is resonant angular frequency of the electron spin precession, and L is a factor of spin delocalization over a polaron equal approximately to five monomer units in P3AT [51, 78].

The dynamic parameters calculated from Eqs.(12) and (13) for both charge carriers in some polymer/fullerene composites are presented in Figure 8 as a function of photon energy and temperature. The dynamics coefficients seem from the Figure to depend on the photon energy $h\nu_{ph}$. These parameters obtained for the $P3AT_{12}$/PCBM composite demonstrate monotonic dependence on $h\nu_{ph}$. On the other hands, nonmonotonic dependence of D_{1D} and D_{3D} on $h\nu_{ph}$ is characteristic for polarons photoinduced in the $P3AT_6$/PCBM composite. The extremas of these functions lie near those (2.0 and 3.1 eV) obtained above for other LEPR parameters. This fact proves additionally the existence of domains with different orderings and sensitivity to their respective light photons in the polymer/fullerene composite.

Polarons photoinduced in the $P3AT_6$/PCBM system demonstrate a sharper $D_{1D}(T)$ dependence than those photoinduced in the $P3AT_{12}$/PCBM composite (Figure 8b). This can be explained, e.g., by the stronger interaction of these charge carriers with lattice phonons in the former matrix and can be described in the framework of the Kivelson-Heeger model [88]

of charge carrier scattering in the lattice of an ordered conjugated polymer matrix. According to this model, if polarons interact with the lattice optical phonons interact with energy E_{ph}, the rate of their diffusion should depend on temperature as [88, 89]

$$D_{1D}(T) = D_{1D}^{0} T^{2} \left[\sinh\left(\frac{E_{ph}}{k_B T} \right) - 1 \right]. \quad (14)$$

Figure 8 shows that the experimental dependences $D_{1D}(T)$ obtained for both the initial and annealed $P3AT_6$/PCBM composites are well approximated by Eq.(14) with E_{ph} presented in Table 4.

The remainder dynamics data presented in Figure 8b can be explained in the frames of the Elliot model based on carrier hopping over the energetic barrier E_b [90]. This model predicts the frequency and temperature dependent diffusion of a charge carrier with a coefficient

$$D_{1,3D,rot}(\omega_e T) = D_{1,3D,rot}^{0} T^{2} \omega_e^{s} \exp\left(\frac{E_b}{k_B T} \right), \quad (15)$$

where the exponent $s = 1 - ck_BT/E_b$ reflects the dimensionality of the system and c is a constant. The values of E_b and c were obtained for, e.g., lightly doped poly(3-methylthiophene) ($P3AT_1$) to be 1.1 eV and 6, respectively [91].

Table 4. The E_{ph} and E_b values (all in eV) determined from Eqs.(14) and (15), respectively, for radical pairs photoinduced by white light in the initial and annealed $P3AT_6$/PCBM composite as well as by laser beam with different photon energy $h\nu_{ph}$ in the $P3AT_{12}$/PCBM system.

	Composite									
	$P3AT_6$/PCBM				$P3AT_{12}$/PCBM					
	Initial		Annealed		$h\nu_{ph}$= 1.88 eV		$h\nu_{ph}$= 2.22 eV		$h\nu_{ph}$= 2.75 eV	
Radical Parameter	$P^{+\bullet}$	$mC_{61}^{-\bullet}$	$P^{+\bullet}$	$mC_{61}^{-\bullet}$	$P^{+\bullet}$	$mC_{61}^{-\bullet}$	$P^{+\bullet}$	$mC_{61}^{-\bullet}$	$P^{+\bullet}$	$mC_{61}^{-\bullet}$
E_{ph}	0.034		0.021							
E_b		0.032		0.007	0.048	0.017	0.038	0.010	0.094	0.012

The energies E_b required to activate polaron longitudinal and fullerene pseudorotational diffusion in the P3AT/PCBM composites is also presented in Table 4. It is seen in Figure 8 that the temperature dependences calculated from Eq.(15) with the E_b obtained approximate well the data determined experimentally. The E_b obtained for fullerene is less considerably as compared with that estimated for fullerene libration in more crystalline solids [92].[93, 94],

However, it is close to that characteristic for triphenylamine complex [95, 96]. The respective barrier height passed by polarons photoinduced in $P3AT_{12}$/PCBM bulk heterojunctions lie near the energy of lattice phonons in $P3AT_8$ [66, 67] and other conjugated polymers [55-57]. It also close to the activation energy E_a of polaron mobility in $P3AT_6$ [97] but less than E_a determined for polaron diffusion in the $P3AT_1$ matrix [98] and in the $P3AT_8$/PCBM composite [99].

Comparing the data obtained, one can conclude that the polaron motion in the P3AT/PCBM composites is definitely governed by their polymer matrix. Indeed, the rate of fullerene pseudorotation decreases in P3AT by some orders of magnitude as the length of its alkyl substitute A increases, i.e., at transfer from $P3AT_6$ to $P3AT_{12}$ matrix. This probably makes it possible to control the main electronic properties of such plastic solar cells by variation of their structure, conformation, and composition. The thermal treatment of the samples also changes their main electronic properties. Such modification reduces the anisotropy of polaron diffusion (see Fig. 8) and both the E_{ph} and E_b values in the $P3AT_6$/PCBM composite (see Table 4). This is evidence of the increase in crystallinity of the treated system. Besides, at the temperature annealing of the composite with initially low-crystalline polymer matrix the fullerene molecules embedded become more mobile and start to diffuse and form fullerene clusters. Due to such thermally initiated fullerene diffusion, the regions with low fullerene concentration appear in the polymer matrix where the polymer macromolecules can crystallize. As a result, polymer crystallites and fullerene clusters are formed upon annealing of the initial composite. Such treatment indeed improves additionally charge transport properties of the P3AT/PCBM and other polymer/fullerene solar cells.

6. CONCLUSION

Light excitation of the bulk heterojunction in the polymer/fullerene composite leads to charge separation and transfer from a polymer chain to a fullerene globule. This is accompanied by the excitation of two paramagnetic centers with rhombic symmetry and clearly resolved LEPR spectra, namely the positively charged polaron $P^{+\bullet}$ on the polymer backbone and the negatively charged fullerene anion radical $mC_{61}^{-\bullet}$ situated between polymer chains. Both radicals are spatially separated due to high mobility of a polaron charge carrier, so that they become noninteracting and the probability of their recombination decreases. Some of these charge carriers may be trapped in the polymer matrix. Weak interaction of paramagnetic centers in this radical pair stipulates a difference in their interaction with their own microenvironment and, therefore, in their magnetic and relaxation parameters. Both radicals are spatially separated due to the high mobility of the polaron charge carrier, so that they become noninteracting and the probability of their recombination decreases. Spatial separation due to delocalization of a charge over fullerene globule reduces additionally the recombination rate of these long-living charge carriers. Weak interaction of paramagnetic centers in the former radical pair stipulates a difference in their interaction with their own microenvironment and, therefore, in their magnetic-resonance parameters. This allows determining separately all relaxation parameters for both charge carriers.

Photoinduced charge is transferred by polaron diffusion along a polymer chain near the position of a fullerene radical anion where they can recombine. The probability of the

collapse of photoinduced radical pairs follows the activation law and is governed by the energy of initiating optical photons. The interaction of charge carriers with their own microenvironment also depends on the photon energy. Spin dynamics induces an additional magnetic field in the whereabouts of other spins that accelerates electron relaxation of both spin ensembles. This allowed all dynamic parameters of polarons and fullerene radical anions in the polymer/fullerene composite to be calculated separately. Q1D longitudinal diffusion of polarons and librational diffusion of fullerenes follow the activation mechanism and are governed by the photon energy. This can be a result of the formation of identical excitations in heterogeneous domains of the system. The temperature annealing of the composite enhances its dimensionality (crystallinity) due to the formation of polymer crystallites and fullerene clusters that improves the main electronic properties of plastic solar cells.

The LEPR study described contributes to a better understanding of the correlations between the structure, magnetic, and transport properties of polymers and their composites with fullerene. Such direct correlations seem to be useful for a further optimization of the polymer/fullerene solar cells. Thus, the gained knowledge about processes carried out in bulk heterojunction of a polymer/fullerene composite is of great importance from both fundamental and engineering points of view. For enhanced transport and carrier generation in these systems the network morphology of the phase-separated composite material should be optimized; light absorption and the mobility of the charge carriers within the different components of the bulk heterojunction have to be maximized as well. It was demonstrated above that the magnetic, relaxation, and dynamics properties of the paramagnetic centers photoinduced in a composite are governed by the energy of excited photons. This can be due to the formation in the system of charge carriers with different properties in a homogeneous composite or identical spin pairs in heterogeneous domains. In the first case the difference in the photon energy can lead to the formation of traps with different depths in a polymer matrix. The other situation seems to be more realistic when the variety in properties of inhomogeneously distributed domains gives rise to a variation in the main properties of charge carriers. Therefore, the investigation of the properties of paramagnetic centers excited by various photons in the initial and treated polymer/fullerene systems may give a possibility to control their texture and other structural properties of solar cells for the further increase in their efficiency factor. An analogous investigation of polymer/fullerene composites at millimeter wavebands EPR (at higher electron precession frequency) will supply us by more detailed information for in-depth elucidation of fundamental electronic processes carrying out in plastic solar cells. Such studies are currently in progress in our laboratory.

7. ACKNOWLEDGMENTS

The author gratefully thanks Professor H.-K. Roth and Professor V.A. Smirnov for the fruitful discussions. This work was in part supported by the Russian Foundation for Basic Researches (Grant No 08-03-00133) and the Human Capital Foundation (Grant No 27-02-5).

8. REFERENCES

[1] Sariciftci, NS; Heeger, AJ. In *Handbook of Organic Conductive Molecules and Polymers*; H. S. Nalwa, (Ed.), John Wiley & Sons: Chichester, New York, 1997, Vol. 1, pp. 413-455.

[2] *Organic Photovoltaic: Concepts and Realization*; C. Brabec, V. Dyakonov, J. Parisi, N. S. Sariciftci, (Eds.), Springer Series in Materials Science; Springer: Berlin, 2003, *Vol. 60*, pp -297.

[3] *Organic Photovoltaics: Mechanisms, Materials, and Devices (Optical Engineering)*; S.-S. Sun, N. S. Sariciftci, (Eds.), Optical Science and Engineering Series; CRC Press: Boca Raton, 2005, *Vol. 99*, pp 1-664.

[4] *Handbook of Conducting Polymers*; T. E. Scotheim, J. R. Reynolds, (Eds.), CRC Press: Boca Raton, 2007, *Vol. 1-2*, pp 1-1680.

[5] Winder, C; Sariciftci, NS. *J. Mater. Chem.*, 2004, *14*, 1077-1086.

[6] *Thin Film Solar Cells: Fabrication, Characterization and Applications*; J. Poortmans, V. Arkhipov, (Eds.), Wiley: West Sussex, 2006, *Vol.* pp -502.

[7] Gunes, S; Neugebauer, H; Sariciftci, NS. *Chem. Rev.*, 2007, *107*, 1324-1338.

[8] Guenes, S; Sariciftci, NS. *Inorgan. Chim. Acta*, 2008, *361*, 581-588.

[9] Zhu, Z; Muhlbacher, D; Morana, M; Koppe, M; Scharber, MC; Waller, D; Dennler, G; Brabec, CJ. In *High-Efficient Low-Cost Photovoltaics*; Springer Series in Optical Sciences; Springer-Verlag: Berlin, Heidelberg, 2009, Vol. pp. 195-222.

[10] Li, G; Shrotriya, V; Huang, JS; Yao, Y; Moriarty, T; Emery, K; Yang, Y. *Nature Mater.*, 2005, *4*, 864-868.

[11] Ma, WL; Yang, CY; Gong, X; Lee, K; Heeger, AJ. *Adv. Funct. Mater.*, 2005, *15*, 1617-1622.

[12] Green, R; Morfa, A; Ferguson, AJ; Kopidakis, N; Rumbles, G; Shaheen, SE. *Appl. Phys. Lett.*, 2008, *92*, 033301-033303.

[13] Shaheen, SE; Brabec, CJ; Sariciftci, NS; Padinger, F; Fromherz, T; Hummelen, JC. *Appl. Phys. Lett.*, 2001, *78*, 841-843.

[14] Brabec, CJ; Padinger, F; Hummelen, JC; Janssen, RAJ; Sariciftci, NS. *Synth. Met.*, 1999, *102*, 861-864.

[15] Shaheen, SE; Radspinner, R; Peyghambarian, N; Jabbour, GE. *Appl. Phys. Lett.*, 2001, *79*, 2996-2998.

[16] Ishikawa, T; Nakamura, M; Fujita, K; Tsutsui, T. *Appl. Phys. Lett.* 2004, *84*, 2424-2426.

[17] Marumoto, K; Muramatsu, Y; Kuroda, S. *Appl. Phys. Lett.*, 2004, *84*, 1317-1319.

[18] Marumoto, K; Muramatsu, Y; Takeuchi, N; Kuroda, S. *Synth. Met.*, 2003, *135*, 433-434.

[19] Sensfuss, S; Al-Ibrahim, M; Konkin, A; Nazmutdinova, G; Zhokhavets, U; Gobsch, G; Egbe, DAM; Klemm, E; Roth, H-K. In *Organic Photovoltaics IV*; Z. H. Kafafi; P. A. Lane, (Eds.), Proceedings of SPIE; 2004, *Vol. 5215*, pp. 129-140.

[20] Al Ibrahim, M; Roth, HK; Schrődner, M; Konkin, A; Zhokhavets, U; Gobsch, G; Scharff, P; Sensfuss, S. *Org. Electron.*, 2005, *6*, 65-77.

[21] Sensfuss, S; Konkin, A; Roth, H-K; Al-Ibrahim, M; Zhokhavets, U; Gobsch, G; Krinichnyi, VI; Nazmutdinova, GA; Klemm, E. *Synth. Met.,* 2003, *137*, 1433-1434.
[22] Krinichnyi, VI; Roth, HK; Sensfuss, S; Schrődner, M; Al Ibrahim, M. *Physica E,* 2007, *36*, 98-101.
[23] Krinichnyi, VI. *Acta Mater.,* 2008, *56*, 1427-1434.
[24] Krinichnyi, VI. *Sol. Energy Mater. Sol. Cells,* 2008, *92*, 942-948.
[25] Krinichnyi, VI; Yudanova, EI. *J. Renew. Sustain. Energy,* 2009, *1*, 043110-1-043110-18.
[26] Krinichnyi, VI; Yudanova, EI; Denisov, NN. *J. Chem. Phys.,* 2009, *131*, 044515-1-044515-11; See also publications at http://hf-epr.sitesled.com/publications.htm
[27] Wang, C; Guo, ZX; Fu, S; Wu, W; Zhu, D. *Prog. Polym. Sci.,* 2004, *29*, 1079-1141.
[28] Sariciftci, NS. *Prog. Quant. Electr.,* 1995, *19*, 131-159.
[29] Hwang, IW; Soci, C; Moses, D; Zhu, ZG; Waller, D; Gaudiana, R; Brabec, CJ; Heeger, AJ. *Adv. Mater.,* 2007, *19*, 2307-2312.
[30] Lee, CH; Yu, G; Moses, D; Pakbaz, K; Zhang, C; Sariciftci, NS; Heeger, AJ; Wudl, F. *Phys. Rev. B,* 1993, *48*, 15425-15433.
[31] Kraabel, B; Lee, CH; McBranch, D; Moses, D; Sariciftci, NS; Heeger, AJ. *Chem. Phys. Lett.,* 1993, *213*, 389-394.
[32] Brabec, CJ; Zerza, G; Cerullo, G; DeSilvestri, S; Luzatti, S; Hummelen, JC; Sariciftci, NS. *Chem. Phys. Lett.,* 2001, *340*, 232-236.
[33] Kraabel, B; McBranch, D; Sariciftci, NS; Moses, D; Heeger, AJ. *Phys. Rev. B,* 1994, *50*, 18543-18552.
[34] Halls, JM; Cornil, J; Dos Santos, DA; Silbey, R; Hwang, DH; Holmes, AB; Bredas, JL; Friend, RH. *Phys. Rev. B,* 1999, *60*, 5721-5727.
[35] Brabec, CJ; Winder, C; Sariciftci, NS; Hummelen, JC; Dhanabalan, A; van Hal, PA; Janssen, RAJ. *Adv. Funct. Mater.,* 2002, *12*, 709-712.
[36] Brabec, CJ; Cravino, A; Meissner, D; Sariciftci, NS; Fromherz, T; Rispens, MT; Sanchez, L; Hummelen, JC. *Adv. Funct. Mater.,* 2001, *11*, 374-380.
[37] Koster, LJA; Mihailetchi, VD; Ramaker, R; Blom, PWM. *Appl. Phys. Lett.,* 2005, *86*, 123509.
[38] Koster, LJA; Mihailetchi, VD; Blom, PWM. *Appl. Phys. Lett.,* 2006, *88*, 093511-093513.
[39] Krinichnyi, VI; Troshin, PA; Denisov, NN. *J. Chem. Phys.,* 2008, *128*, 164715-1-164715-7.
[40] Krinichnyi, VI; Troshin, PA; Denisov, NN. *Acta Mater.,* 2008, *56*, 3982-3989.
[41] Lenes, M; Wetzelaer, G-JAH; Kooistra, FB; Veenstra, SC; Hummelen, JC; Blom, PWM. *Adv. Mater.,* 2008, *20*, 2116-2119.
[42] Bassler, H. *Phys. Stat. Solidi B,* 1993, *175*, 15-56.
[43] Montanari, I; Nogueira, AF; Nelson, J; Durrant, JR; Winder, C; Loi, MA; Sariciftci, NS; Brabec, C. *Appl. Phys. Lett.,* 2002, *81*, 3001-3003.
[44] Sariciftci, NS; Smilowitz, L; Heeger, AJ; Wudl, F. *Science,* 1992, *258*, 1474-1476.
[45] Brabec, CJ; Dyakonov, V; Sariciftci, NS; Graupner, W; Leising, G; Hummelen, JC. *J. Chem. Phys.,* 1998, *109*, 1185-1195.
[46] Frolov, SV; Lane, PA; Ozaki, M; Yoshino, K; Vardeny, ZV. *Chem. Phys. Lett.,* 1998, *286*, 21-27.

[47] Nogueira, AF; Montanari, I; Nelson, J; Durrant, JR; Winder, C; Sariciftci, NS. *J. Phys. Chem. B,* 2003, *107*, 1567-1573.
[48] Dyakonov, V; Zoriniants, G; Scharber, M; Brabec, CJ; Janssen, RAJ; Hummelen, JC; Sariciftci, NS. *Phys. Rev. B,* 1999, *59*, 8019-8025.
[49] Juska, G; Arlauskas, K; Sliauzys, G; Pivrikas, A; Mozer, AJ; Sariciftci, NS; Scharber, M; Osterbacka, R. *Appl. Phys. Lett.,* 2005, *87*, 222110-1-222110-3.
[50] Leng, JM; McCall, RP; Cromack, KR; Ginder, JM; Ye, HJ; Sun, Y; Manohar, SK; MacDiarmid, AG; Epstein, AJ. *Phys. Rev. Lett.,* 1992, *68*, 1184-1187.
[51] Westerling, M; Osterbacka, R; Stubb, H. *Phys. Rev. B,* 2002, *66*, 165220-1-165220-7.
[52] *Solitons and Polarons in Conducting Polymers*; Y. Lu, (Ed.), World Scientific: River Edge, NJ, Singapore, 1988, pp. 1-772.
[53] Mizoguchi, K; Kuroda, S. In *Handbook of Organic Conductive Molecules and Polymers*; H. S. Nalwa, (Ed.), John Wiley & Sons: Chichester, New York, 1997, *Vol. 3*, pp. 251-317.
[54] Bernier, P. In *Handbook of Conducting Polymers*; T. E. Scotheim, (Ed.), Marcel Deccer, Inc.: New York, 1986, *Vol. 2*, pp. 1099-1125.
[55] Krinichnyi, VI. *2-mm Wave Band EPR Spectroscopy of Condensed Systems*; CRC Press: Boca Raton, 1995, pp. 1-223.
[56] Krinichnyi, VI. *Synth. Met.,* 2000, *108*, 173-222.
[57] Krinichnyi, VI. In *Advanced ESR Methods in Polymer Research*; S. Schlick, (Ed.), Wiley: Hoboken, NJ, 2006, pp. 307-338.
[58] Janssen, RAJ; Moses, D; Sariciftci, NS. *J. Chem. Phys.,* 1994, *101*, 9519-9527.
[59] Konkin, AL; Sensfuss, S; Roth, HK; Nazmutdinova, G; Schrődner, M; Al Ibrahim, M; Egbe, DAM. *Synth. Met.,* 2005, *148*, 199-204.
[60] Pivrikas, A; Sariciftci, NS; Juska, G; Osterbacka, R. *Prog. Photovolt.,* 2007, *15*, 677-696.
[61] Al-Ibrahim, M; Roth, H-K; Zhokhavets, U; Gobsch, G; Sensfuss, S. *Sol. Energy Mater. Sol. Cells,* 2004, *85*, 13-20.
[62] Qiao, XY; Wang, XH; Mo, ZS. *Synth. Met.,* 2001, *118*, 89-95.
[63] van Hal, PA; Wienk, MM; Kroon, JM; Verhees, WJH; Slooff, LH; van Gennip, WJH; Jonkheijm, P; Janssen, RAJ. *Adv. Mater.,* 2003, *15*, 118-121.
[64] Sensfuss, S; Al-Ibrahim, M. In *Organic Photovoltaics: Mechanisms, Materials, and Devices (Optical Engineering)*; S.-S. Sun; N. S. Sariciftci, (Eds.), Optical Science and Engineering Series; CRC Press: Boca Raton, 2005, pp. 529-557.
[65] Mőbius, K. *Z. Naturforsch. A,* 1965, *20A*, 1093-1102.
[66] Krinichnyi, VI; Roth, HK; Konkin, AL. *Physica B,* 2004, *344*, 430-435.
[67] Krinichnyi, VI; Roth, H-K. *Appl. Magn. Reson.,* 2004, *26*, 395-415.
[68] Eaton, SS; Eaton, GR. *Appl. Magn. Reson.,* 1996, *11*, 155-170.
[69] De Ceuster, J; Goovaerts, E; Bouwen, A; Hummelen, JC; Dyakonov, V. *Phys. Rev. B,* 2001, *64*, 195206-1-195206-6.
[70] Allemand, PM; Srdanov, G; Koch, A; Khemani, K; Wudl, F; Rubin, Y; Diederich, F; Alvarez, MM; Anz, SJ; Whetten, RL. *J. Amer. Chem. Soc.,* 1991, *113*, 2780-2781.
[71] Dubois, D; Jones, MT; Kadish, KM. *J. Amer. Chem. Soc.,* 1992, *114*, 6446-6451.
[72] Boyd, PDW; Bhyrappa, P; Paul, P; Stinchcombe, J; Bolskar, RD; Sun, YP; Reed, CA. *J. Amer. Chem. Soc.,* 1995, *117*, 2907-2914.
[73] Tosatti, E; Manini, N; Gunnarsson, O. *Phys. Rev. B,* 1996, *54*, 17184-17190.

[74] Bietsch, W; Bao, J; Ludecke, J; van Smaalen, S. *Chem. Phys. Lett.*, 2000, *324*, 37-42.
[75] Krinichnyi, VI; Pelekh, AE; Lebedev, YS; Tkachenko, LI; Kozub, GI; Barra, AL; Brunel, LC; Robert, JB. *Appl. Magn. Reson*., 1994, *7*, 459-467.
[76] Nelson, J. *Phys. Rev. B*, 2003, *67*, 155209-1-155209-10.
[77] Tanaka, H; Hasegawa, N; Sakamoto, T; Marumoto, K; Kuroda, SI. *Japan. J. Appl. Phys*., 2007, *46*, 5187-5192.
[78] Devreux, F; Genoud, F; Nechtschein, M; Villeret, B. In *Electronic Properties of Conjugated Polymers*; H. Kuzmany; M. Mehring; S. Roth, (Eds.), Springer Series in Solid State Sciences; Springer-Verlag: Berlin, 1987, *Vol. 76*, pp. 270-276.
[79] Houze, E; Nechtschein, M. *Phys. Rev. B*, 1996, *53*, 14309-14318.
[80] Molin, YN; Salikhov, KM; Zamaraev, KI. *Spin Exchange*; Springer Series in Chemical Physics; Springer-Verlag: Berlin, 1980, *Vol. 8*, pp. 111-115.
[81] Krinichnyi, VI; Roth, H-K; Schroedner, M; Wessling, B. *Polymer*, 2006, *47*, 7460-7468.
[82] Krinichnyi, VI; Tokarev, SV; Roth, H-K; Schroedner, M; Wessling, B. *Synth. Met.*, 2006, *156*, 1368-1377.
[83] Krinichnyi, VI; Grinberg, OY; Nazarova, IB; Kozub, GI; Tkachenko, LI; Khidekel, ML; Lebedev, YS. *Bull. Acad. Sci. USSR, Div. Chem. Sci.*, 1985, *34*, 425-427.
[84] Schultz, NA; Scharber, MC; Brabec, CJ; Sariciftci, NS. *Phys. Rev. B*, 2001, *64*, 245210-1-245210-7.
[85] Poole, ChP. *Electron Spin Resonance, A Comprehensive Treatise on Experimental Techniques*; John Wiley & Sons: New York, 1983.
[86] Krinichnyi, VI; Pelekh, AE; Tkachenko, LI; Kozub, GI. *Synth. Met.*, 1992, *46*, 1-12.
[87] Carrington, F; McLachlan, AD. *Introduction to Magnetic Resonance with Application to Chemistry and Chemical Physics*; Harrer & Row, Publishers: New York, Evanston, London, 1967.
[88] Kivelson, S; Heeger, AJ. *Synth. Met.*, 1988, *22*, 371-384.
[89] Pietronero, L. *Synth. Met.*, 1983, *8*, 225-231.
[90] Long, AR; Balkan, N. *Philos. Magaz. B*, 1980, *41*, 287-305.
[91] Parneix, JP; El Kadiri, M. In *Electronic Properties of Conjugated Polymers*; H. Kuzmany; M. Mehring; S. Roth, (Eds.), Springer Series in Solid State Sciences; Springer-Verlag: Berlin, 1987, *Vol. 76*, pp. 23-26.
[92] Chow, PC; Jiang, X; Reiter, G; Wochner, P; Moss, SC; Axe, JD; Hanson, JC; McMullan, RK; Meng, RL; Chu, CW. *Phys. Rev. Lett.*, 1992, *69*, 2943-2946.
[93] Firlej, L; Kuchta, B; Roszak, S. *Synth. Met.*, 1998, *94*, 77-81.
[94] Morosin, B; Hu, ZB; Jorgensen, JD; Short, S; Schirber, JE; Kwei, GH. *Phys. Rev. B*, 1999, *59*, 6051-6057.
[95] Denisov, NN; Krinichnyi, VI; Nadtochenko, VA. In *Fullerenes. Recent Advances in the Chemistryand Physics of Fullerenes and Related Materials*; K. Kadish; R. Ruoff, (Eds.), The Electrochemical Society Inc.: Pennington, 1997, *Vol. 97-14*, pp. 139-147.
[96] Denisov, NN; Krinichnyi, VI; Nadtochenko, VA. *Chem. Phys. Rep*., 1998, *17*, 1405-1415.
[97] Chiguvare, Z; Dyakonov, V. *Phys. Rev. B*, 2004, *70*, 235207-1-235207-8.
[98] Tagmouti, S; Outzourhit, A; Oueriagli, A; Khaidar, M; Elyacoubi, M; Evrard, R; Ameziane, EL. *Sol. Energy Mater. Sol. Cells*, 2002, *71*, 9-18.
[99] Krinichnyi, VI; Demianets, YN; Mironova, SA. *Physica E*, 2008, *40*, 2829-2833.

LbL composites display performance parameters 10-1000 times better that the traditional nanocomposites made by extrusion or batch-mixing.Â In addition to mechanical properties, polymer nanocomposites based on carbon nanotubes or graphene have been used to enhance a wide range of properties, giving rise to functional materials for a wide range of high added value applications in fields such as energy conversion and storage, sensing and biomedical tissue engineering.[22] For example, multi-walled carbon nanotubes based polymer nanocomposites have been used. for the enhancement of the electrical conductivity.[23].Â A range of polymeric nanocomposites are used for biomedical applications such as tissue Applications of Polymer Composites. 2. P.E. 406 Polymer Composites.Â Composites ï‚¢ Increased awareness regarding product performance and increased competition in the global market for lightweight components fueled their growth. ï‚¢ Among all materials, composite materials have the potential to replace widely used steel and aluminum, and many times with better performance.Â Continuous & Short Fiber Composites ï‚¢ The properties strongly depend on the way the fibers are laid in the composite. ï‚¢ The important thing to remember about composites is that the fiber carries the load and its strength is greatest along the axis of the fiber. ï‚¢ Long continuous fibers in the direction of the load result in a composite with properties far exceeding the matrix resin. The present chapter covers the designing, development, properties and applications of carbon nanotube-loaded polymer composites. The first section will provide a brief overview of carbon nanotubes (CNTs), their synthesis, properties and functionalization routes. The second section will shed light on the CNT/polymer composites, their types, synthesis routes and characterization.Â Open access peer-reviewed chapter. Carbon Nanotube-Based Polymer Composites: Synthesis, Properties and Applications. By Waseem Khan, Rahul Sharma and Parveen Saini. Submitted: October 20th 2015Reviewed: February 12th 2016Published: July 20th 2016.